



An Experimental Study of a Two-Phase Closed Thermosyphon Rankine Cycle Performance

دراسة عملية لأداء سيفون حراري ذو الطورين مغلق يتبع دورة رانكن

A.R. Habieeb, G.I. Sultan, M.M. Awad and A.R. Elshmouty

KEYWORDS:

Thermosyphon, Rankine turbine, low temperature, revolution per minute.

الملخص العربي: إن تقليل الحرارة المزالة لأي دورة توليد طاقة هو عامل واعد في تحسين الأداء العام وتقليل الاحتباس الحراري. يمكن القيام بذلك بطرق مختلفة مثل المبادلات الحرارية أو السيفون الحراري. استخدمت الدراسة التجريبية الحالية الماء كسائل ناقل للحرارة، وتم دراسة نسبة الملاء (9% ≤ Fr) ، ومساحة خروج الفوهة الكلية إلى مساحة مدخل التوربين (Ar ≤ 4.343)، وماء تبريد الداخل للمكثف معدل التدفق (8 LPM ≥ V). أظهرت النتائج أن نسبة الملاء المثلى تبلغ حوالي 13.6% وزادت طاقة الإنتاج مع زيادة معدل تدفق ماء التبريد المكثف. أيضًا، تنتج طاقة الخرج القصوى بأقل نسبة للمنطقة، لكن السرعة الدورانية التوربينية المثلى عند نسبة مساحة قدرها 3.1%. بالإضافة إلى ذلك، تبلغ أقصى طاقة خرج بدون تحميل من التوربين الحالي Fr=16 LPM ، W 5.28 ، Ar=2.5%

Abstract— Decreasing the heat rejection of any power cycle is a promising agent in improving the overall performance and decreasing global warming. This can be done by different methods such as heat exchangers or thermosyphons. Water is used as a working fluid. The present experimental work used water as a working fluid and investigated the effects of filling ratio (27.2% ≥ Fr ≥ 9%), total nozzle exit area to the turbine inlet area (4.3% ≥ Ar ≥ 2.5%), and condenser cooling water flow rate (16 LPM ≥ V) ≥ 8 LPM). The results showed that the optimum-filling ratio is approximately 13.6% and the output power increases with increasing condenser cooling water flow rate. Also, the maximum output power produced at minimum area ratio but the optimum turbine rotational speed at area ratio of 3.1%. In

addition, the maximum output power without load from the present turbine is 5.28 W at Fr= 13.6 %, Ar=2.5% and V =16 LPM.

Nomenclature

| | |
|------------|---|
| A_o | Total nozzles exit area, m ² |
| Ar | Area ratio, % |
| A_s | Surface area of the insulator, m ² |
| B | The amplitude |
| d_n | Total nozzles diameter, m |
| D_s | Outer diameter of insulator, m |
| F | The vibration frequency |
| Fr | The volume of working fluid to the total volume of thermosyphon Rankine engine, % |
| H | Heat transfer coefficient of convection, W/m ² . K |
| h_{fg} | The change of specific enthalpy from saturated liquid to saturated vapor in the condition of the evaporator, J/kg |
| I | Current, Amperes |
| L | Length, m |
| L_s | The length of the evaporator and adiabatic section |
| \dot{m} | The rate of mass flow of vapor, kg/s |
| N | The turbine rotational speed, rpm |
| P | The produced power of thermosyphon Rankine engine, W |
| \dot{Q} | The heat transfer rate in the evaporator section, W |
| Q_{loss} | The heat losses in evaporator and adiabatic section |
| q | The heat flux |

Received: (13 October, 2019) - Revised: (6 January, 2020) - Accepted: (12 January, 2020)

A.R. Habieeb, a Demonstrator at the Department of Basic Engineering, Faculty of Engineering, Delta University for Science and Technology, Gamasa, Egypt (e-mail: abedrabiee@gmail.com).

G.I. Sultan, a Professor at the Department of Mechanical Power Engineering, Mansoura University, Mansoura, Egypt (e-mail: gisultan@mans.edu.eg).

M.M. Awad, an Associate Professor at the Department of Mechanical Power Engineering, Mansoura University, Mansoura, Egypt (e-mail: m_m_awad@mans.edu.eg).

A.R. Elshmouty, a Lecturer at the Department of Basic Engineering, Faculty of Engineering, Delta University for Science and Technology, Gamasa, Egypt (e-mail: dr.ahmed@deltauniv.eg)

| | |
|------------------------------|---|
| R | Radius of the rotor, m |
| T | Temperature, °C |
| T_s | Surface temperature of insulator |
| T_∞ | Ambient temperature |
| U | The velocity of the nozzle, m/s |
| V | Voltages, volts |
| \dot{V} | Condenser cooling water flow rate, LPM |
| V_a | The absolute velocity of the vapor with respect to stationary observer, m/s |
| V_r | The exit relative velocity of vapor with respect to the rotor, m/s |
| V^+ | Filling ratio, volume of the working fluid to the evaporator volume [3] |

Greek symbols

| | |
|----------------------------|--|
| ρ_o | The density of the vapor leaving the nozzle, kg/m ³ |
| τ | The torque produced by the fluid flow through the rotor, Nm |
| ω | Turbine angular velocity, rad/s |
| Φ | The phase angle between voltage and current, degree |

I. INTRODUCTION AND LITERATURE REVIEWS

THE thermosyphon is widely used in many industries due to its simple structure, light device with no moving parts, high efficiency and simple working mechanism. In addition, a large amount of heat can be transferred with very small temperature difference between the heat source (evaporator section) and the heat sink (condenser section). Heat applied to the evaporator section of the pipe causes the working fluid to evaporate which then moves to the condenser section of the pipe, releasing the heat absorbed during the evaporation, condenses back to the liquid form and the condensed fluid then return back to the evaporator section.

Due to their high efficiency, reliability, and cost effectiveness, thermosyphons have been used in many different applications

Shrhaan et al., [1] presented an experimental and theoretical study on the flow and heat transfer performance of the two-phase offset and elbow thermosyphons. For offset thermosyphon experiments were performed to investigate the effect of heat flux, filling ratio, inclination angle, ratio between condenser to evaporator length, and offset length on the performance of two-phase closed thermosyphon. They used water as the working fluid. Their experiments were carried out for the values of heat flux of 7.35, 13.8, 22.0, and 28.3 kW/m². The values of the operating filling ratios were 25%, 50%, 75%, 100%, and 125%. The values of the inclination angles were -15°, 0° (vertical position), 15°, 30°, and 45° measured from the vertical axis. The values of offset length were 100, 130, and 180mm. Three different values of the ratio between condenser to evaporator length of 3, 1.5, and 1 were used. For elbow (L) thermosyphon, experiments were performed to investigate the effect of the filling ratio, and the ratio between condensers to evaporator length, at vertical position.

Shalaby et al., [2] presented an experimental study on the heat transfer performance of low temperature two-phase closed thermosyphon. Experiments are performed to investigate the effect of the heat flux, the filling ratio (volume of the working fluid to the evaporator volume), and the

inclination angle on the performance of low temperature two-phase closed thermosyphon. They used R22 as a working fluid. The operating heat fluxes are 2526.3, 5052.5 and 7578.8 W/m². The values of the operating filling ratios were 100%, 80%, 60%, 50%, 40%, and 30%. The values of the inclination angles were 90° (vertical position), 60°, 45°, 37.5°, 30°, 22.5° measured from the horizontal level. Their results indicated that the maximum performance is obtained at an inclination angle of 30°, and the optimum filling ratio is found to be 50%.

Shalaby et al., [3] presented an experimental and theoretically work to study the heat transfer performance of a vertical two-phase closed thermosyphon. R134a is used as a working fluid. The present work studied the influence of the filling ratio ($30\% \leq V^+ \leq 100\%$), the heat flux ($1276 \text{ W/m}^2 \leq q \leq 6331 \text{ W/m}^2$), dimensionless amplitude ($0.19 \leq B \leq 0.57$), and dimensionless frequency ($1.08 \leq F \leq 3.26$) on the heat transfer of a two-phase closed thermosyphon. Their results showed that the optimum-filling ratio is 50% approximately. Also, the vibration enhanced the thermosyphon performance by 5 to 18.8% approximately and the amplitude led to enhance the thermosyphon performance by 5.5 to 10.5 %.

Tchuen and Kohole [4] performed a numerical investigation to study the performance of three various thermosyphon with water heating system. The flat-plate solar collectors considered are the absorber-pipe lower bond configuration (Type I), the absorber-pipe side bond configuration (Type II) and the absorber-pipe upper bond configuration (Type III). The average values of the energetic and exergetic efficiencies: 39.47% and 18.21% for Type I, 34.86% and 15.45% for Type II, 32.28% and 13.8% for Type III.

Merzha et al., [5] enhanced the performance of flat plate solar collector using the heat pipe. The experimental test is represented by twisting portion of the evaporator section and also inclined by an angle of 30° with a constant total length of 114 cm. In this work the evaporator, adiabatic and condenser lengths are 78 cm, 14 cm and 23 cm respectively. The omitted energies from sun light simulator are 200, 400, 600, 800 and 1000 W/m² which is close to the normal solar energy in Iraq. The working fluid for all models is water with fill charge ratio of 30%. Three values of condenser inlet water temperatures, namely (12°, 16° and 20° C) are used in the experiments. Their results showed that the radiation incident increases the overall heat transfer coefficient of thermosyphon is increases. Also, the performance of solar collector with twisted evaporator greater than other types of evaporator as a ratio 13.5 %.

Ozsoy and Corumlu [6] presented an experimental study to investigate the effect of nanofluids on the performance of thermosyphon heat pipe (THP) evacuated tube solar collector. The silver-water nanofluid was used in this study. Their results observed that the use of silver-water nanofluid gives a significant heat transfer enhancement in the THP evacuated tube solar collector. In addition to, nanofluid enhanced the efficiency of solar collector between 20.7% and 40% compared with the pure water.

Gorecki [7] studied the thermal performance of a two-phase thermosyphon with modern HFC refrigerants. In the present work three refrigerants were tested: R134a, R404A and R407C. The total length of tube was 55 cm with equal length (24.5 cm) condenser and evaporator sections its external diameter is 22 mm and internal diameter 20 mm. Results showed that the optimum filling ratio was 10 % based on the total volume of the tube. R134a and R404A performance was 50% higher than R407C.

Heat Pipe Turbine is a new concept for power generation from solar, geothermal or other available low-grade heat sources. It uses a modification of the thermosyphon cycle, which has good heat and mass transfer characteristics, and incorporates a turbine in the adiabatic section. The configuration involves a closed, vertical cylinder functioning as an evaporator, an insulated section and a condenser (shown in Fig.1).

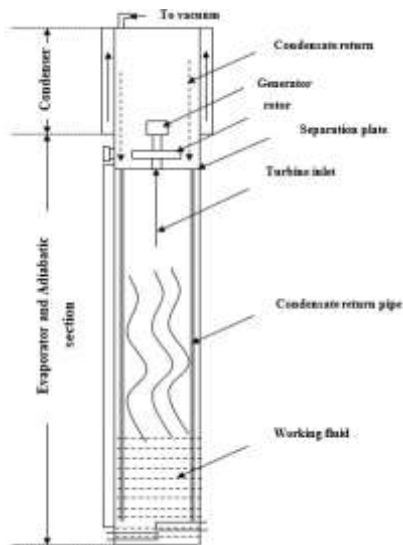


Fig. 1 Schematic diagram of a heat pipe turbine

The turbine is placed near the upper end between the insulated section and a condenser section; a plate is installed to separate the high-pressure region from the low-pressure region in the condenser. Conversion of the fluid enthalpy to kinetic energy is achieved through a nozzle. The mechanical energy developed by the turbine can be converted by direct coupling to an electrical generator. The working fluid is placed in the evaporator section of the heat pipe and flows to the upper section after evaporation. The condenser is located in the upper section. Here the vapor transforms into liquid again and the condensate returns to the evaporator section by gravity force. Between the evaporator and the condenser, the vapor passes through the rotor. There were multiple models of TSR were built at RMIT (Royal Melbourne Institute of Technology), where the initial rig was built at in approximately 1994 was housed in a vertically oriented, sealable copper tube measuring 2.9m tall with a 0.16m external diameter, Nguyen et al., [8]. The combined length of the evaporator and adiabatic sections measured 2.0m (at rest, the working fluid level was 0.5m) while the condenser section

measured 0.9m long. During testing, using water as the working fluid, the first TSR ran with an evaporating temperature of 60° and condensing temperature of 30°C (operating under vacuum conditions). Producing a very modest electrical output, the turbine rotated at speeds between 600 and 800 rpm. A hydrostatic head of 1.7m (of the 2.0m possible) was recorded which displays that 85% of the maximum pressure difference for the unit was achieved. The second TSR was redesigned to accommodate a higher mass flow rate (2000 times the previous setup) by increasing the nozzle size and improving the turbine blade profiles. It was observed from the experimental results that the second prototype had a relatively large temperature difference between the heat source fluid and the working fluid in the evaporator (15°C) indicating a reasonably high thermal resistance there. Despite this handicap, the unit was able to achieve a 2kW heat transfer rate, with 9.0% of this being lost in transport across the heat pipe. The turbine generated power over a speed range of approximately 1750 to 3350 rpm and had a maximum electrical output of 0.35W at 2540 rpm. Although this represents an overall efficiency of 0.175%, it showed progress in the development of the TSR with the higher rotational speeds obtained and a measurable production of electricity.

The third TSR was designed to improve the overall efficiency of the heat pipe-turbine while also reducing production costs. The closed vertical cylinder (3.15m) had an external diameter of 0.16m and heights of 0.5m, 1.7m and 0.9m for the evaporator, adiabatic and condenser sections respectively. An increased heat transfer rate of 4.4 kW was calculated for the evaporator. The maximum turbine speed increased to approximately 5600 rpm and a peak electrical output of 4.5W was obtained at around 4800 rpm. It can be seen from the results that the design aims of the rotor in third TSR had been met in terms of increased heat input, simplicity, lack of expense and higher achievable rotational speeds. The overall conversion efficiency of the third TSR, however, was actually less than the second prototype at 0.125%. The fourth prototype was again a revised design and this time it was made from transparent acrylic to allow visual inspection of all of the heat pipe operation. The evaporator section measured 0.5m, the adiabatic 1.7m and the condenser section measured 0.7m in length. It was decided to set the inside diameter at 0.5m in order to lower the rotational speed of the rotor whilst retaining the possibility of increasing the power output (due to increased torque). This model was tested and produced electricity at various evaporator temperatures from 44°C to 55°C. Tests were conducted to gather data that would allow for a range of heat source temperatures and varying heat exchanger effectiveness. Although the Carnot efficiencies start at 7.3%, (for 42°C evaporator temperature) and climb to 10.7% (for the 55°C run), the overall efficiencies achieved display a much greater spread. The overall conversion achieved was 0.2% for the 42°C run and up to 0.81% for the 55°C evaporator temperature, showing significantly higher overall conversion efficiencies in this region (efficiency quadrupled). It is impossible to con-sider separately the effect of the rotor and

the generator in this setup. Using data from an earlier investigation into the operating characteristics of the Maxon DC generator, indications are that the majority of the improvement in overall conversion efficiency can be contributed to the generator running in its preferred speed band. The minority of the overall efficiency increase would seem to be contributed from the increase in the turbine's isentropic efficiency during the higher temperature runs. Nonetheless, a more than 6-fold increase in the overall conversion efficiency gained by the fourth TSR over the third was the most significant improvement achieved and showed further potential. The fifth TSR was primarily designed by Akbarzadeh et al., [9] this experimental test further simplified the design for ease of manufacturing and cost effectiveness. The rotor consists of a hub with two 'S' shaped pipes connected to it. The water vapor flows upward through the hub, and the direction of flow is varied to horizontal while entering the two pipes on the periphery. Then the water vapor flows through the two pipes and leaves through the nozzle at the pipe outlets, causing the reaction force which drives the turbine. The heat added for this turbine is 100 KW at 58 °C and it is expressed to produced 3 KW of electrical output power the aim of this project is to investigate experimentally the performance of the TSR engine by designing a new model, where there are a very limited number of TSR models that have been investigated.

Ziapour [10] had developed a looped where vapor and liquid flow passage are separated by installing liquid feeding tube with showering nozzle. He enhanced the design of the TSR system using an impulse turbine. In his paper energy and exergy analysis of TRC was formulated in order to estimate its optimum operating conditions, his results showed that his present model can be able to increase the efficiency of the TSR system. Ziapour et al., [11] In their work they improved the loop type TSR system by adding super heating process. The system drum (or pool) type evaporator had been selected instead of the showering nozzle type evaporator where this type of evaporator can be suitable for receiving the renewable energy need via the flow boiling process.

Elshamy [12] presented an experimental study on the performance of thermosyphon Rankine engine as a low temperature heat engine. The thermosyphon tube, which was

used in his study, was made of a copper tube (21 cm outside diameter, 19.5 cm inside diameter, 1.4 m length, the evaporator and adiabatic section length of 0.8 m, and the condenser section length of 0.6 m. He made turbine blades from aluminum material and consist of 8 blades. Turbine set-up comprised two nozzles with an inner and outer diameter 3mm & 7mm respectively. The two-return pipe of condensed fluid are made from copper with 5 mm diameter each. A 24V DC electrical generator was coupled above the turbine. His results indicated that as the input power increase the all temperature gradient increase, as the input power increase the output power will increase, and the efficiency of the TSR decrease as the output power increase because of the mechanical losses. Also, his study showed that at 1000-W input power the output power was 0.056 W approximately and 0.07% maximum efficiency was obtained.

From the previous literature review, a very little work are done in this area of study. So, the aim of the present study is to investigate experimentally the performance of the two-phase closed thermosyphon Rankine engine. The present experimental work investigated the effects of the filling ratio ($27.2\% \geq Fr \geq 9\%$), total nozzle exit area to the turbine inlet area ($4.3\% \geq Ar \geq 2.5\%$), and condenser cooling water flow rate ($16\text{LPM} \geq \dot{V} \geq 8\text{LPM}$), on the TSR performance.

II. EXPERIMENTAL PROCEDURES

The experimental test rig shown in Fig. (2) has been designed and constructed specially for the present work. It consists of a galvanized steel tube, an electric heater, a constant head tank, a turbine that is based on the Hero reaction turbine principle, and measurement devices. The thermosyphon tube is made of a galvanized steel with 0.33m inside diameter, 3-mm thickness, and 2.2 m total length. The thermosyphon consists of three sections. The lower section, 0.6 m long, constitutes the evaporator, the middle section, 1.1 m long represents the adiabatic section, and the third section of 0.5 m long, constitutes the condenser section. The turbine is located near the upper end between the adiabatic section and a condenser section as shown schematically and photography in Fig (3).

1. Cooling water pump
2. Tank inlet water
3. Cooling water tank
4. Float valve
5. Tank drain
6. Condenser water inlet
7. Flow meter
8. Thermometer
9. Condenser water outlet
10. Electric heater
11. Turbine
12. Condensate return
13. Viewing port
14. Tachometer
15. Vacuum pump
16. Pressure gage
17. Thermocouple
18. Temperature recorder
19. Voltmeter
20. Ammeter
21. Single phase electric source
22. A vertical graduated clear tube

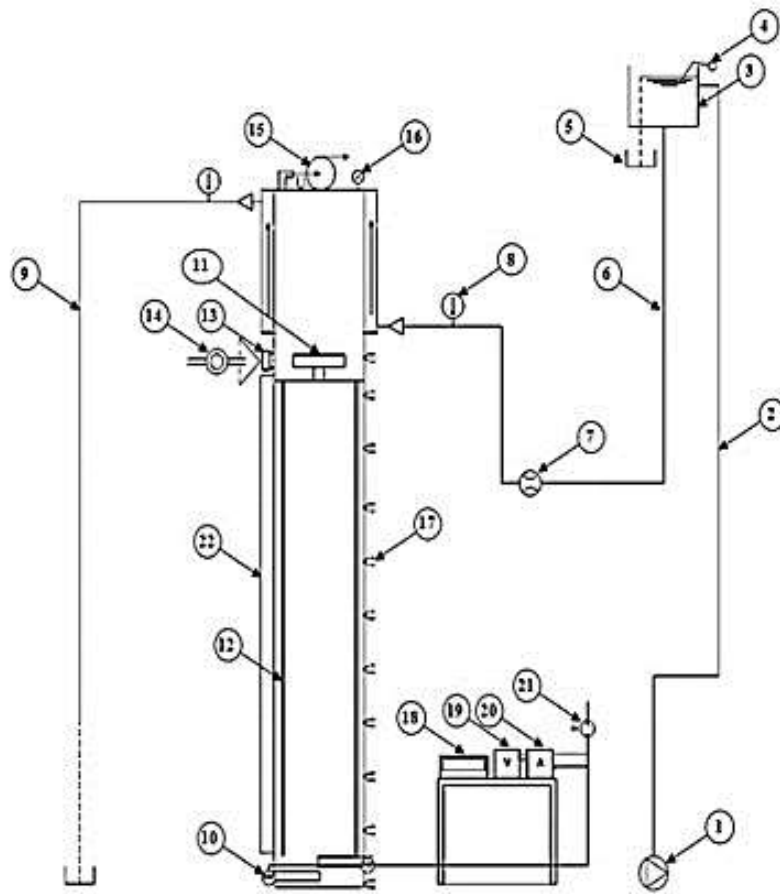


Fig. 2 Schematic diagram of a thermosyphon test rig

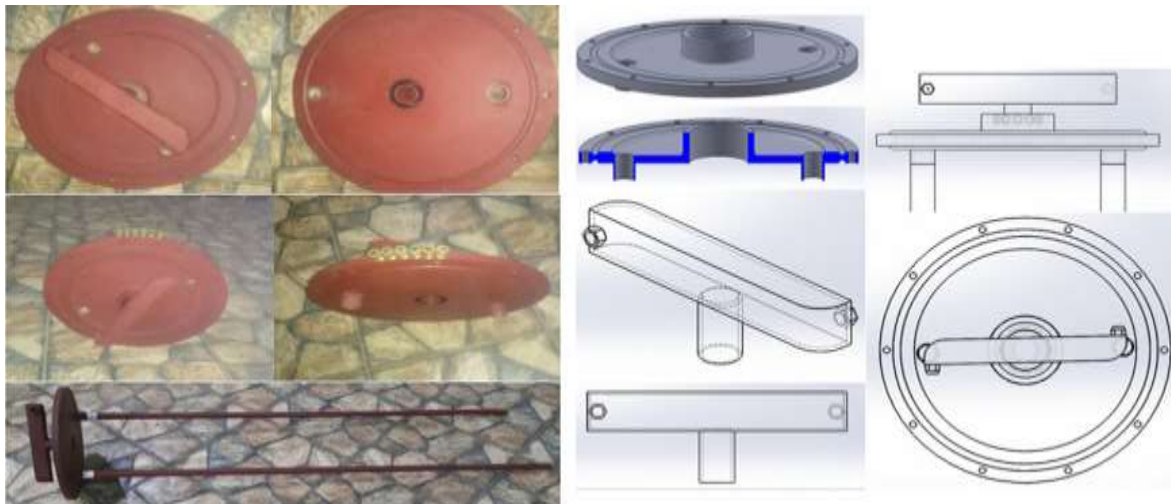


Fig. 3 Rotor and its base

A plate is installed to separate the high-pressure section from the low-pressure section in the condenser.

The rotor is based on the Hero reaction turbine principle and was made as economically as practicable by using readily available square hollow section and two variable copper nozzles and hub. The rotor arms were principally made from one-piece aluminum, fixed within the hub by bearing, and

with a central opening oriented downwards to receive the vapor stream.

Water is used as a working fluid. The evaporator section is heated by the two electric heaters 5 kW for each one. The electric heater is made of a nickel chrome strip. The first heater is placed at 5 cm from the bottom of thermosyphon and

the other on is placed the other side at 15 cm from the bottom of thermosyphon.

To reduce the heat loss from the thermosyphon tube, the evaporator and adiabatic section are covered with glass wool insulation (40 mm thick). A number of 12 thermocouples type-K are used to measure the temperature distribution along the outer surface of the thermosyphon tube. Each of them is glued at equal spacing along the evaporator and adiabatic section, and the last thermocouple glued on the top of condenser section. The thermocouples attached to temperature recorder model (Digi-Sense Thermocouple Scanning Thermometer with 12-Channels). The accuracy in the temperature measurement is about ± 0.5 °C. Two mercury thermometers are used to measure the temperature of cooling water at the inlet and outlet of the condenser. The condenser section is cooled by water that flows through an annular water jacket. The cooling jacket of condenser is made of steel, 0.33m inside diameter, 0.38m outside diameter and 0.5m length. The cooling jacket and the thermosyphon tube are assembled by two-flange. A constant level water head tank is obtained using float valve, which mounted on the water inlet of the tank. The total head of supply water is 3 m above the cooling water inlet. The flow rate of condenser cooling water is controlled by a valve and is measured by a flowmeter.

The pressure gauge is mounted on the top of the thermosyphon tube (-1:15 bar) to measure the vacuum pressure inside the thermosyphon with an expected error ± 0.05 bar and the vacuum pump is used to evacuate the system. The condenser cooling water flowrate is measured by the flowmeter that its range from (2-18) LPM with an error ± 0.1 .

An A.C electrical power source of 220V is used to supply the required power to the heaters. The input power can be calculated by measuring the applied voltage on the heaters by the voltmeter, and the electric current passing through them by using an ammeter. Turbine speed is measured by an analog handheld tachometer (CEM DT-6234B), its range from (2.5 to 99,999) RPM. It measures RPM value using the laser beam reflection from the reflex tape stucked on the measured object. The expected error in the turbine speed measurement is ± 0.1 RPM.

III. DATA PROCESSING

Experiments are performed to investigate the effect of filling ratio; turbine exit area and cooling water flow rate on both turbine rotational speed and output power. In this section how to find the produced power from turbine speed measured in practice.

The input power is calculated from the following equation:

$$\dot{Q} = IV \cos \phi, \cos \phi = 1 \quad (1)$$

The rate of mass flow of vapor generated in the evaporator is then:

$$\dot{m} = \frac{\dot{Q}}{h_{fg}} \quad (2)$$

The exit relative velocity of water vapor from the rotor with respect to the nozzle is calculated by the following equation:

$$V_r = \frac{\dot{m}}{\rho \cdot A_0} \quad (3)$$

The velocity at the nozzle of reaction turbine is determined by:

$$U = R\omega \quad (4)$$

The absolute velocity of the water vapor with respect to fixed point will be given by:

$$V_a = V_r - U \quad (5)$$

The fluid flow through the rotor produces the torque that given by:

$$\tau = \dot{m} V_a R \quad (6)$$

The out power can be calculated as:

$$P = \tau \omega = \dot{m} V_a R \omega \quad (7)$$

Filling ratio, Fr is calculated from:

$$Fr = \frac{V_{working\ fluid}}{V_{thermosyphon}} * 100\% \quad (8)$$

Area ratio, Ar is calculated from:

$$A_r = \frac{Total\ nozzels\ exit\ area}{Turbine\ inlet\ area} * 100\% \quad (9)$$

IV. ERROR ANALYSIS

The maximum expected relative error in calculating the out power is 3.5% as given by [3]

$$P = f(T, L, \dot{V}, Fr, \tau, \omega)$$

$$\left| \frac{\delta P}{P} \right| = \sqrt{\left(\frac{\Delta T}{T}\right)^2 + \left(\frac{\Delta L}{L}\right)^2 + \left(\frac{\Delta \dot{V}}{\dot{V}}\right)^2 + \left(\frac{\Delta Fr}{Fr}\right)^2 + \left(\frac{\Delta \tau}{\tau}\right)^2 + \left(\frac{\Delta \omega}{\omega}\right)^2}$$

V. RESULTS AND DISCUSSIONS

The experimental work is used to study the temperature distribution along TSR and effect of filling ratio, turbine exit area and cooling water flow rate on both turbine rotational speed and exit power

Temperature Distribution along the Thermosyphon

The temperature values are recorded along the thermosyphon tube wall for all tests in the region of $0.0 < x < 2.5$ m, where x is measured from the evaporator base.

Figure (4) shows the temperature distribution along the axial direction of the thermosyphon tube for the area ratio of 3.1 %, condenser cooling water flow rate 16 LPM, and different filling ratio. It can be observed that the temperature slight decrease up to $x = 1.5$ m from the evaporator base and then decreases along the condenser section. From Fig (4), it indicated that the filling ratio doesn't affect on the temperature distribution along the axial direction of the thermosyphon tube.

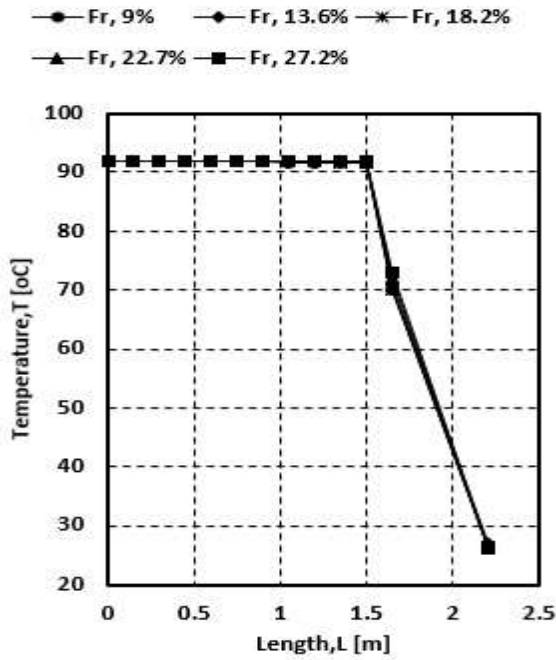


Fig. 4 The temperature distribution along the length at different filling ratio

Figure (5) shows the temperature distribution along the axial direction of the thermosyphon tube for the filling ratio of 13.6%, condenser cooling water flow rate 16 LPM, and different area ratio. It can be observed that the temperature slight decrease up to $x = 1.5$ m from the evaporator base and then decreases along the condenser section. From Fig (5), it indicated that the area ratio effects on the temperature distribution at the turbine section (1.5-2) m.

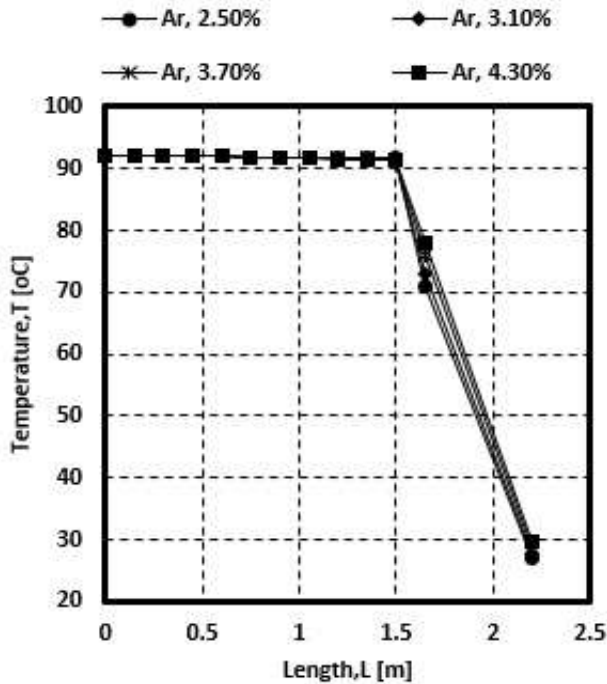


Fig. 5 The temperature distribution along the length at different rea ratio

Figure (6) shows the temperature distribution along the axial direction of the thermosyphon tube for the Area ratio of 3.1 %, filling ratio 13.6 %, and different condenser cooling water flow rate. It can be observed that the temperature slight decrease up to $x = 1.5$ m from the evaporator base and then decreases along the condenser section. From Fig (6), it indicated that the condenser cooling water has insignificant effect on the temperature distribution along the axial direction of the thermosyphon tube.

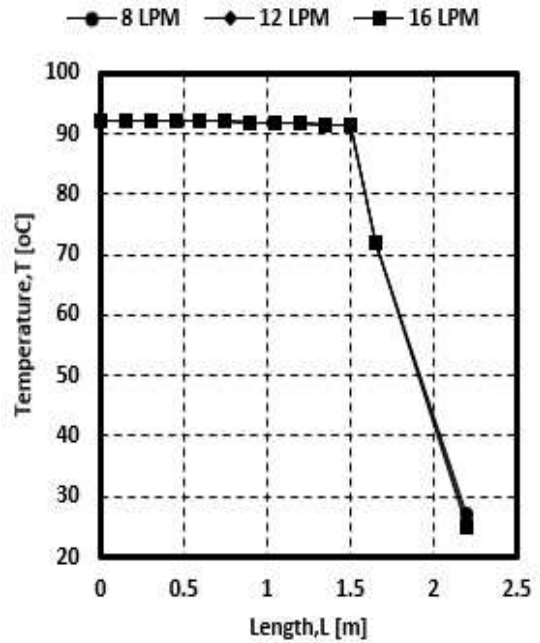


Fig. 6 The temperature distribution along the length at different condenser cooling water flow rate

Effect of the Filling Ratio

Figure (7) shows the variation of the output power (P) with the filling ratio (Fr) at area ratio of 2.5 % and different condenser cooling water flowrate. The figure shows that the output power increases with increasing filling ratio until reaches a certain value after which the output power dramatically decreases. For example, at $Fr = 13.6\%$, and $Ar = 2.5\%$, the output power is about $P = 4.91$ W. at $V = 8$ LPM, $P = 5.11$ W. at $V = 12$ LPM, and $P = 5.28$ W. at $V = 16$ LPM.

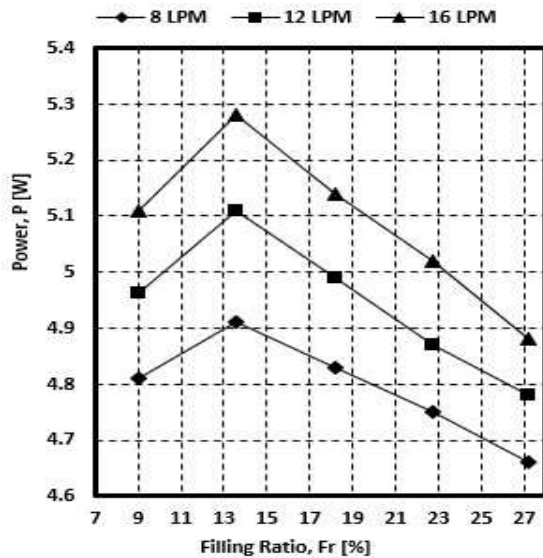


Fig. 7 The output power versus the filling ratio at different values of condenser cooling water flow rate and area ratio 2.5%

Figure (8) shows the variation of the output power (P) with the filling ratio (Fr) at condenser cooling water flowrate 16 LPM and different area ratio. The figure indicated that the output power increases with increasing filling ratio until reaches a maximum value. Far from this value the output power decreases.

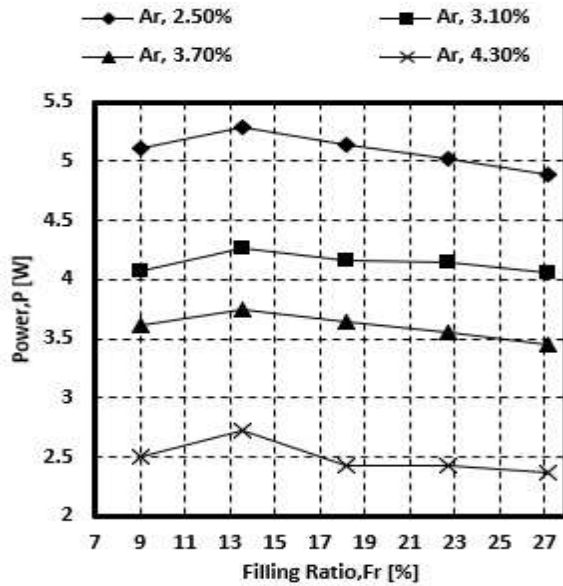


Fig. 8 The output power versus the filling ratio at different values of area ratio and condenser cooling water flow rate 16LPM

Effect of the nozzle exit area on the power

Figure (9) shows the effect of area ratio of the turbine on output power at condenser cooling water flow rate 16LPM, and different filling ratio. It is observed that by increasing the area ratio the output power from the thermosyphon Rankine (TSR) engine decreases. The maximum value of output power P= 5.28 W at area ratio Ar= 2.5 %, filling ratio Fr= 13.6 %, and condenser cooling water V = 16LPM.

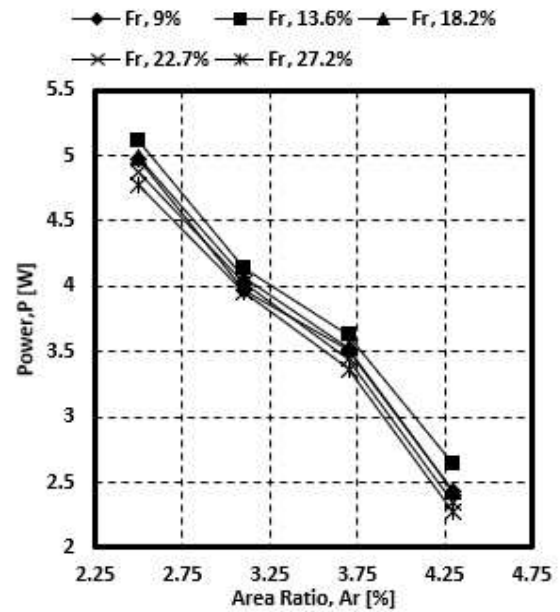


Fig. 9 The output power versus the area ratio at different values of filling ratio and condenser cooling water flow rate 16LPM

Figure (10) shows the effect of the area ratio of turbine on output power at filling ratio 13.6%, and different condenser cooling water flow rate. It is observed that by increasing the area ratio the output power of the thermosyphon Rankine (TSR) engine decreases

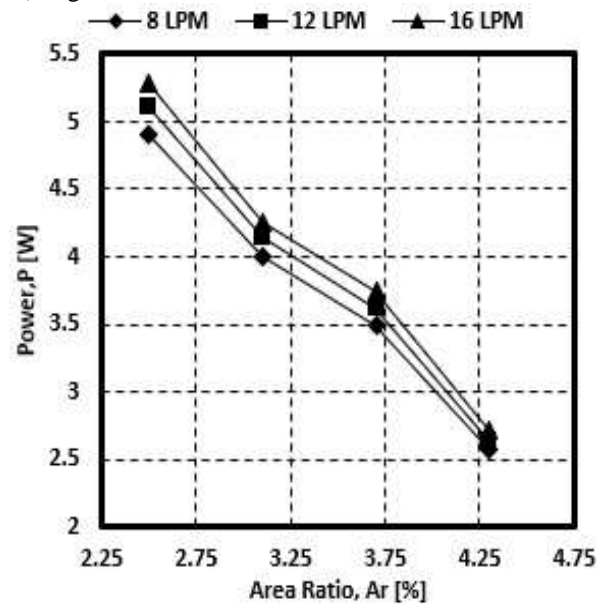


Fig. 10 The output power versus the area ratio at different values of condenser cooling water flow rate and filling ratio 13.6%

Effect of the nozzle exit area on the RPM

Figure (11) shows the variation of the turbine rotational speed with the area ratio at filling ratio 13.6%, and different condenser cooling water flowrate. It is clear that, the area ratio 3.1 % gives maximum value of the turbine rotational speed. Far from this value the output power decreases. For

example, at $Ar=3.1\%$, and $Fr=13.6\%$, the turbine rotational speed is about $N=375\text{rpm}$. at $V=8\text{LPM}$, $N=388\text{rpm}$. at $V=12\text{LPM}$, and $N=400\text{rpm}$. at $V=16\text{LPM}$.

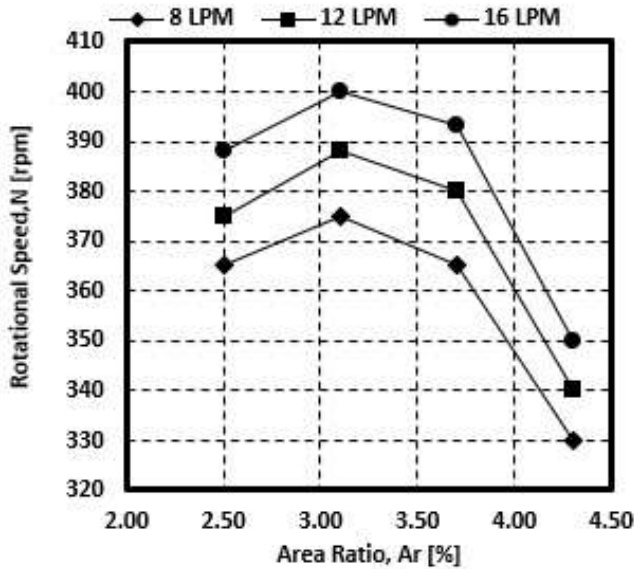


Fig. 11 The rotational speed versus the area ratio at different values of condenser cooling water flow rate and filling ratio 13.6%

Figure (12) shows the variation of the turbine rotational speed with the area ratio at condenser cooling water flow rate 16LPM, and different filling ratio. It is obvious that, the area ratio of 3.1% gives maximum value of the turbine rotational speed. Far from this value the output power decreases

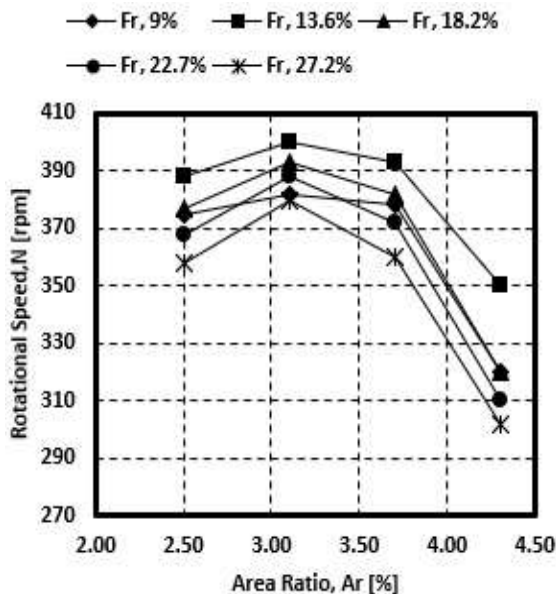


Fig. 12 The rotational speed versus the area ratio at different values of filling ratio and condenser cooling water flow rate 16LPM

Effect of the cooling water flowrate

Figure (13) shows the effect of the cooling water flow rate on the output power of thermosyphon Rankine engine (TSR) at a different area ratio, and filling ratio 13.6%. The figure

declared that with increasing the cooling water flow rate the output power increases.

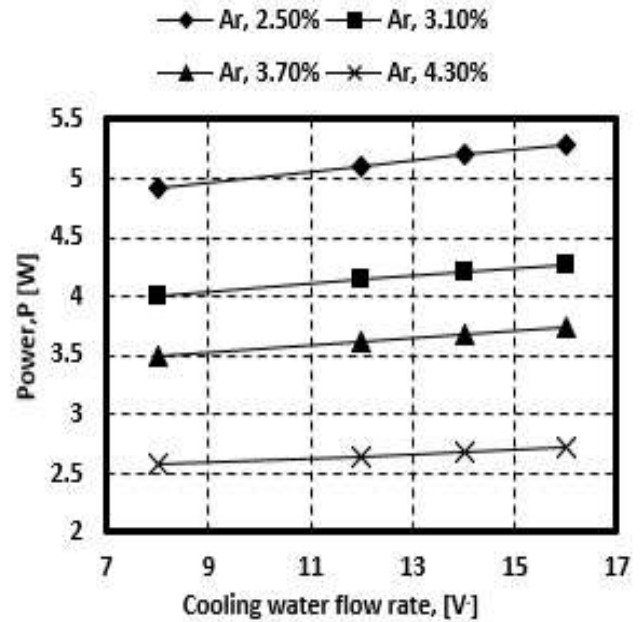


Fig. 13 The output power versus the condenser cooling water flow rate at different values of area ratio and filling ratio 13.6%

Figure (14) shows the effect of the cooling water flow rate on the output power of thermosyphon Rankine engine (TSR) at a different filling ratio, and area ratio 2.5%. The figure clear that with increasing the cooling water flow rate the output power increases.

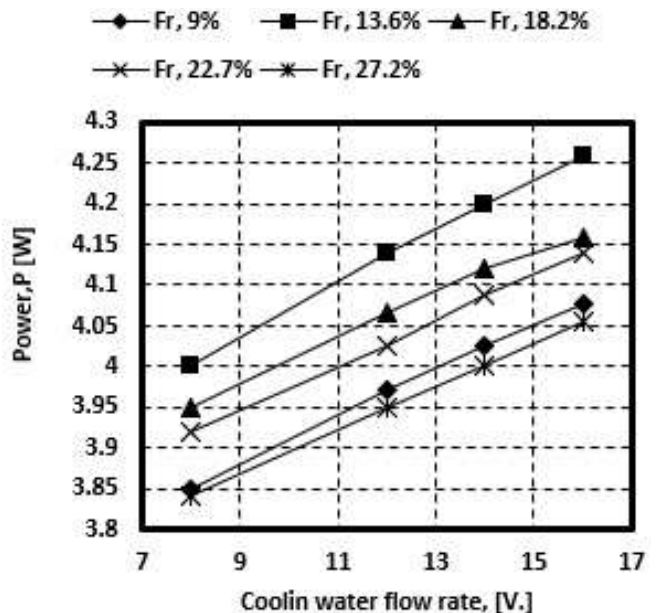


Fig. 14 The output power versus the condenser cooling water flow rate at different values of filling ratio and area ratio 2.5%

VI. CONCLUSION

The purpose of this study is to investigate the performance of a two-phase closed thermosyphon Rankine engine, experimentally. Water is used as a working fluid.

The present experimental work investigated the effects of the filling ratio ($9\% \leq Fr \leq 27.2\%$), total nozzle exit area to the turbine inlet area ($2.5\% \leq Ar \leq 4.3\%$), and condenser cooling water flow rate ($8 \leq \dot{V} \leq 16 \text{ LPM}$).

The conclusions of the present study are: -

- The optimum-filling ratio is 13.6% approximately
- The output power increases with increasing of condenser cooling water flow rate.
- The maximum output power produced at minimum area ratio but the optimum turbine rotational speed at an area ratio of 3.1%.
- The maximum value of the output power without load from the present turbine is 5.28 W at $Fr = 13.6\%$, $Ar = 2.5$ and $\dot{V} = 16 \text{ LPM}$.

REFERENCES

- [1] Sarhaan H. H., "Flow and Heat Transfer in Wickless Heat Pipe", Ph.D Thesis, Mansoura University, September 2000
- [2] Shalaby M. A., Araid F. F., Sultan G. I., and Awad M. M., "Heat Transfer Performance of a Two-Phase Closed Thermosyphon", The 6th International Engineering Research, El-Azhar, 2000.
- [3] A. A. A. Hegazi, M. A. Shalaby, and G. I. Sultan " Heat transfer performance of a vibrated two-phase closed thermosyphon ", MEPCON, Mansoura, May 2003.
- [4] Ghislain Tchuen, Wenceslas Yemeli Kohole, "A numerical investigation of three different thermosyphon solar water heating systems", International Journal of Ambient Energy, (2018), No. 6, p. 637-48.
- [5] Basil N. Merzha, Majid H. Majeed, Fouad A. Saleh, "Experimental study of flat plate solar collector performance with twisted heat pipe", IOP Conference Series: Materials Science and Engineering, (2019), p. 032035 (12 pp.).
- [6] Ahmet Ozsoy, Vahit Corumlu, "Thermal performance of a thermosyphon heat pipe evacuated tube solar collector using silver-water nanofluid for commercial applications", Renewable Energy, (2018), p. 26-34.
- [7] Grzegorz Gorecki, "Investigation of two-phase thermosyphon performance filled with modern HFC refrigerants", Heat and Mass Transfer, (2018), no. 7, p. 2131-43.
- [8] T.Nguyen, P. Johnson, A. Akbarzadeh, K. Gibson and M. Mochizuki, " Design, Manufacture and Testing of a Closed Cycle Thermosyphon Rankine Engine", Heat Recovery Systems & CHP, 15, 1995, No.4, p. 333-346.
- [9] A.Akbarzadeh, P.Johnson, T.Nguyen, M.Mochizuki, M.Mashico, I.Sauciuc, S.Kusaba, H.Suzuki, "Formulation and Analysis Of The Heat Pipe Turbine For Production Of Power From Renewable Sources", Applied Thermal Engineering, (2001), No. 21, p. 1551-1563.
- [10] B.M. Ziapour, "Performance analysis of an enhanced thermosyphon Rankine cycle using impulse turbine", Energy, (2009), No. 34, p. 1636-1641.
- [11] B.M. Ziapour, A. Mohammadnia, M. Baygan, "More about Thermosyphone Rankine Cycle Performance Enhancement", International Journal of Engineering, (2015), No. 4, p. 642-647.
- [12] Samir M. Elshamy, "Performance of Thermosyphon Rankine Engine as Low Temperature Heat Engine", International Journal of Scientific & Engineering Research, (2017), p. 126-130.